Minimum energy route optimisation of a quad-copter UAV with landing incentivisation*

Alexander Blakesley[1], Bani Anvari[1], Jakub Krol[1], Michael G.H. Bell[2]

***Abstract*— Recent advancements in the technology surrounding UAVs have expanded the possibility of incorporating them into current logistical solutions. In order to accurately assess their capabilities, it is important that minimum energy trajectories can be generated to increase the travel range of a UAV as well as its possible number of visited locations. However, in current formulations of the optimisation problem, UAV dynamics does not incorporate a contact force on the ground. This results in hover-to-hover trajectories where the duration of the journey is exactly equal to an arrival time which is set as one of the problem's parameters. Those solutions are likely to be energetically sub-optimal if an unnecessarily large value of arrival time is chosen. This paper introduces landing capability by modifying gravitational acceleration in the dynamics using a sigmoid function which approaches zero at the destination. In this way, the trip can be conducted in a shorter amount of time if it results in lower energy consumption. The new model is compared against an example from the literature, where the corresponding solution results in a reduction of the travel time and energy consumption by approximately 80%. It is also applied to a real-world example where it is demonstrated that a UAV can provide energy savings if it replaces a van completing a delivery in the Solent region of the UK.**

I. INTRODUCTION

A lot of research in recent years has been investigating the use of unmanned aerial vehicles (UAVs) to compliment the current business-as-usual (BAU) of land logistics. In most cases, current BAU consists of diesel vans (DVs) visiting multiple stops along their routes. One of the major advantages of DVs over UAVs is their energy efficiency for short trips, when traffic congestion is low to medium and the drone is required to land frequently to perform drop-offs or pickups. However, in many situations those conditions are not satisfied and when the inverse is true, UAVs can become significantly more efficient than DVs [1].

In order to obtain a greater understanding of where UAVs may be more energy and time efficient than DVs, an accurate evaluation of their capabilities is needed. One of the major obstacles in the utilisation of drones are battery limitations, which constrain their range and the possible number of visited locations [2]. Technological solutions to alleviate these issues include autonomous charging solutions [3], [4], more efficient rotor layouts [5] and solar powered UAV designs [6]. However, these solutions are currently in the prototype stages. Alternative way to maximise the effectiveness of UAVs is to perform trajectory optimisation that aims to minimise their energy consumption. It should be noted that energy minimisation is inadvertently linked to a reduction of travel time [7]. Since energy is consumed when keeping a UAV in the air, through prolonged hover or other maneuvers, a UAV is incentivised to reach its destination and land in a shorter amount of time.

A fundamental issue identified within the literature is the lack of landing capability in the energy route optimisation of UAVs, where solutions are characterised by hover-to-hover trajectories [2], [8], [9]. All of the problem formulations include the gravity force in the description of the UAV's dynamics. However, the contact force on the ground is rarely modelled, and the control input has to be maintained throughout the optimisation's time horizon in order to counteract gravity, leading to increased energy expenditure. As horizontal flight is 2.3% more energy efficient than hovering [10], [11], the UAV only reaches the destination at a pre-specified final time t_f, even though there might exist a trajectory with travel time smaller than t_f that provides greater energy savings. The appropriate choice of t_f is not trivial since low values induce a lack of a feasible solution, whilst large values lead to energetically sub-optimal trajectories.

The contribution of this paper is to supplement the problem formulation by introducing landing capability into the dynamics of the UAV, which ensures it reaches its final destination solely based on considerations of energy efficiency. The proposed model is validated on a theoretical test scenario, compared with a benchmark in the literature and finally evaluated on a real-world test case in the Solent region of the UK by comparing it to the land logistics solution.

The article is organised as follow. Section II summarises the related literature. Section III outlines the UAV dynamics and the modifications introduced that allow for landing. Section IV discusses the minimum energy route optimisation which is evaluated in Section V followed by the discussion of the results in Section VI. Finally, Section VII concludes the paper and outlines future work.

II. RELATED WORK

An initial investigation into the possibility of UAVs becoming a solution for logistics problems was examined in [12], where the energy efficiency of UAVs was analysed to estimate their operating cost and subsequently compared

*This work is financially supported by the Engineering and Physical Sciences Research Council (grant number: EP/V002619/1) and the Department of Civil, Environmental and Geomatic Engineering, University College London, UK.

[1]Alexander Blakesley, Bani Anvari and Jakub Krol are with the Centre for Transport Studies Department of Civil, Environmental and Geomatic Engineering, University College London, Gower Street, United Kingdom, b.anvari@ucl.ac.uk

[2]Michael G.H. Bell is with the Institute of Transport and Logistics, University of Sydney, Australia,

against vans. However, the model excluded many factors such as hovering, vertical flight and empty return capabilities.

In [8] three types of trajectories are developed based on the minimum acceleration, minimum jerk and minimum snap during the route. Their energetic efficiency is evaluated to find that minimum snap trajectories can consume up to 9.4% less than minimum acceleration and 5% less than minimum jerk. In [2] an optimal control problem is solved by minimising a cost function developed using the electric model of a brushless DC model which provides energy consumption for a given angular velocity and acceleration of a propeller. Two problem formulations are provided: 1) minimisation of the energy consumption for a set travel time and 2) travel time minimisation given a set energy budget.

In [10], an energy model is used as an objective function to solve a vehicle routing problem via a simulated annealing heuristic. The model is based on the fundamentals of helicopter flight but does not take into account the effects of wind or avionics. It was compared with empirical data to demonstrate that horizontal flight is more energy efficient than hovering. A more accurate matching to empirical data was achieved in [13] by incorporating wind speed together with effects of drag and lift.

In [1] a model is developed that takes into account more complex avionics like downwash and includes the possibility of empty return payloads in order to compare the energy efficiency of a UAV against a van in logistics services. It is demonstrated that hovering and wind can have a strong effect on the energy consumption, however, the model is not validated using empirical data.

III. APPLIED DYNAMICS OF A QUAD-COPTER UAV

A. Quad-copter Dynamics

A model of a quad-copter can be adapted from helicopter dynamics [14]. Similar formulations are used to represent the dynamics of UAVs in multiple different minimum energy route optimisation problems including [2], [8], [15] and [9]. A quad-copter UAV is modelled as four DC motors on a cross shaped frame of constant arm length, l. The position vector of the UAV, $\boldsymbol{x} = [x, y, z]^\top$, is defined at its center of mass and is relative to the origin, and $\boldsymbol{\phi} = [\phi, \theta, \psi]^\top$ is the rotation vector around the co-ordinate system in the x, y and z direction, also referred to as the roll, pitch and yaw angles. Each motor rotates at an angular velocity, ω_i, $i = 1...4$, with motors 1 and 3 rotating anti-clockwise and 2 and 4 rotating clockwise. The dynamic formulation follows [14] and is given by:

$$\dot{x} = \frac{dx}{dt}, \tag{1}$$

$$\ddot{x} = \frac{T}{m}(\cos\phi\sin\theta\cos\psi + \sin\phi\sin\psi), \tag{2}$$

$$\dot{y} = \frac{dy}{dt}, \tag{3}$$

$$\ddot{y} = \frac{T}{m}(\cos\phi\sin\theta\sin\psi - \sin\phi\cos\psi), \tag{4}$$

$$\dot{z} = \frac{dz}{dt}, \tag{5}$$

$$\ddot{z} = \frac{T}{m}(\cos\phi\cos\theta) - g, \tag{6}$$

$$\dot{\phi} = \frac{d\phi}{dt}, \tag{7}$$

$$\ddot{\phi} = \frac{I_y - I_z}{I_x}\dot{\theta}\dot{\psi} + \frac{(F_2 - F_4)l}{I_x} - \frac{J\dot{\theta}\bar{\omega}}{I_x}, \tag{8}$$

$$\dot{\theta} = \frac{d\theta}{dt}, \tag{9}$$

$$\ddot{\theta} = \frac{I_z - I_x}{I_y}\dot{\phi}\dot{\psi} + \frac{(F_3 - F_1)l}{I_y} + \frac{J\dot{\phi}\bar{\omega}}{I_y}, \tag{10}$$

$$\dot{\psi} = \frac{d\psi}{dt}, \tag{11}$$

$$\ddot{\psi} = \frac{I_x - I_y}{I_z}\dot{\phi}\dot{\theta} + \frac{(M_1 - M_2 + M_3 - M_4)}{I_z}, \tag{12}$$

where $F_i = k_b(\omega_i^2)$, $M_i = k_\tau(\omega_i^2)$, $T = \sum_{i=1}^{4} F_i$, $\bar{\omega} = \omega_1 - \omega_2 + \omega_3 - \omega_4$, m is the mass of the UAV, g is acceleration due to gravity, I_x, I_y, I_z are the components of body inertia, $k_b = C_T\rho A r^2$ is the thrust factor, $k_\tau = C_Q\rho A r^3$ is the drag factor, $A = \pi r^2$ for propeller radius r, ρ is the density of air, C_T is the propeller thrust coefficient, C_Q is the propeller torque coefficient, $J = J_m + J_l$ where the J_m denotes motor moments of inertia and $J_l = \frac{1}{4}n_B m_B(r-e)^2$ is load moment of inertia, n_B is the number of blades on each motor, m_B is the mass of each blade and e is is the offset between the motor center and blade root. The parameter values are given in Table I following [2] and [16] and represent a DJI Phantom 2.

B. Landing Capability

The dynamics of the UAV is modified by enforcing $g = 0$ at a final destination, $\boldsymbol{x}_f = [x_f, y_f, z_f]^\top$, which mimics an introduction of an equal and opposite force to the gravity. In order to ensure that dynamics is differentiable, g is modelled using a modified sigmoid function

$$f(w) = \frac{2}{1 + e^{-kw}} - 1 \tag{13}$$

with a decay rate k. It has a property $f(w) \to 0$ as $w \to 0$ and $f(w) \to 1$ as $w \to \infty$. The rate at which f approaches 0 is given by k. Let $||\Delta\boldsymbol{x}||^2 := (x_f - x)^2 + (y_f - y)^2 + (z_f - z)^2$.

TABLE I: Physical Parameters used to represent the dynamics of a DJI Phantom 2 [2] [16]

m	1.3 kg	g	9.8066 m/s^2
l	0.175 m	I_x	0.081 kgm^2
C_Q	2.3515 x 10^{-4}	I_y	0.081 kgm^2
C_T	0.0048	I_z	0.0142 kgm^2
J_m	4.9 x 10^{-6} kgm^2	r	0.12
ρ	1.225 kgm^3	e	0.004
n_B	2	m_B	0.0055 kg
K_T	$9.5493/K_V$ Vs/rad	K_V	920 rpm/V
T_f	$4 \times 10^{-2} Nm$	R	0.2 Ω
D_f	$2 \times 10^{-4} Nms/rad$	ω_{max}	1000 rad/s

In order to ensure that gravitational acceleration approaches zero at the final destination the gravitational acceleration is modelled as

$$\frac{2g}{1+e^{-k||\Delta \boldsymbol{x}||^2}} - 1. \tag{14}$$

This modification is introduced in (6) such that

$$\ddot{z} = \frac{T}{m}(\cos\phi\cos\theta) - g\left(\frac{2}{1+e^{-k||\Delta \boldsymbol{x}||^2}} - 1\right). \tag{15}$$

The formulation (15) achieves an equilibrium in the vertical direction at a final destination when $T = 0$ and consequently $\omega_i = 0$ which has a potential to reduce energy consumption. In the following analysis $k = 3$, which indicates that an error in gravitational acceleration is less than 10% for $||\Delta \boldsymbol{x}||^2 >$ 1 m. At the same time k is small enough to prevent large change in derivatives.

IV. MINIMUM ENERGY ROUTE OPTIMISATION

The trajectory optimisation of a UAV is formulated as an optimal control problem that minimises energy consumption over the course of a trajectory.

The instantaneous energy E_i associated with the i-th motor is evaluated following an approach given in [2], where

$$\begin{aligned} E_i = \; & \frac{RT_f^2}{K_T^2} + \frac{T_f}{K_T}\left(\frac{2RD_f}{K_T} + K_T\right)\omega_i(t) \\ & + \left(\frac{D_f}{K_T}\left(\frac{RD_f}{K_T} + K_T\right) + \frac{2RT_f k_\tau}{K_T^2}\right)\omega_i^2(t) \\ & + \frac{k_\tau}{K_T}\left(\frac{2RD_f}{K_T} + K_T\right)\omega_i^3(t) \\ & + \frac{Rk_\tau^2}{K_T^2}\omega_i^4(t) \\ & + \frac{RJ^2}{K_T^2}\dot{\omega}_i^2(t) \end{aligned} \tag{16}$$

where K_T is the motor torque constant, K_V is the motor velocity constant, T_f is the motor friction torque, D_f is the motor viscous damping coefficient and R is the resistance of phase winding.

The objective function aims to reduce energy consumption, such that:

$$\min_{\omega_i} \sum_{i=1}^{4} \int_{t_0}^{t_f} E_i \; dt. \tag{17}$$

The state space consists of UAV's position and rotation, as well as their rate of change, i.e.

$$[x, y, z, \dot{x}, \dot{y}, \dot{z}, \phi, \theta, \psi, \dot{\phi}, \dot{\theta}, \dot{\psi}]^\top, \tag{18}$$

whilst control inputs are set to the angular velocity of the four motors

$$[\omega_1, \omega_2, \omega_3, \omega_4]^\top. \tag{19}$$

The dynamics of the UAV is defined by (1) - (12) where (6) is replaced by (15).

Instance constraints are defined at the start of the route, t_0,

$$[x_0, y_0, z_0, 0 \times 9]^\top, \tag{20}$$

and at its end, t_f,

$$[x_f, y_f, z_f, 0 \times 9]^\top. \tag{21}$$

It should be noted that although the constraint for the final location has been specified at t_f, due to the incentives added in (15), the optimiser aims to land at $\boldsymbol{x}_f$ when it is the most energy optimal. Finally, the physical bounds are applied to the problem:

$$\begin{aligned} 0 \leq \omega_i \leq \omega_{max} \\ 0 \leq z \\ -\pi/10 \leq \phi \leq \pi/10 \\ -\pi/10 \leq \theta \leq \pi/10. \end{aligned} \tag{22}$$

The optimisation problem is discretised using the direct collocation method [17], and subsequently solved numerically using the interior point line search filter method as implemented in the IPOPT solver [18]. The problem is discretised using the trapezoidal collocation method into 500 nodes. The acceptable convergence tolerance for the algorithm was set to 10^{-4} and the maximum number of iterations varied depending on the test case.

V. RESULTS

The effectiveness of the proposed model is demonstrated on three test cases:

1) Case 1: A theoretical test case in which the UAV must travel a short distance and land on the ground at its destination.
2) Case 2: A comparative test case which benchmarks the solution against the example from [2].
3) Case 3: A test case based on a real-world example demonstrating the benefit of UAVs in a logistics solution, compared against the land BAU.

A. Case 1: Theoretical Test Case

The validity of the model is tested on a theoretical test case which involves the UAV flying between its origin, $\boldsymbol{x}_0 = [0, 0, 0]^\top$, and final destination, $\boldsymbol{x}_f = [10, 10, 0]^\top$. The final time, t_f is set to 10 s and the maximum iterations was set to 5,000.

Figure 1(a) shows the state trajectories and demonstrates that the UAV lands at its final destination approximately 4 s after t_0, and proceeds to stay stationary for the remainder of the time horizon. It also shows that in x and y, a smooth acceleration period occurs at the start of the trajectory and of deceleration when it approaches the destination such that speed is approximately parabolic. In the z axis, a slightly different trajectory is seen, where the UAV ascends to a peak height of 1.3 m at 2.25 s and then decreases its altitude back to 0 as it approaches its final destination in x and y.

Figure 1(b) demonstrates that variation of ω_i is larger than for the state values. This behaviour is due to the UAV changing its rotation in the direction towards the destination. Once the UAV has reached its destination, it begins to slowly rotate to satisfy its terminal state given by (21), which results in minor changes in ω and z in the latter portion of the time

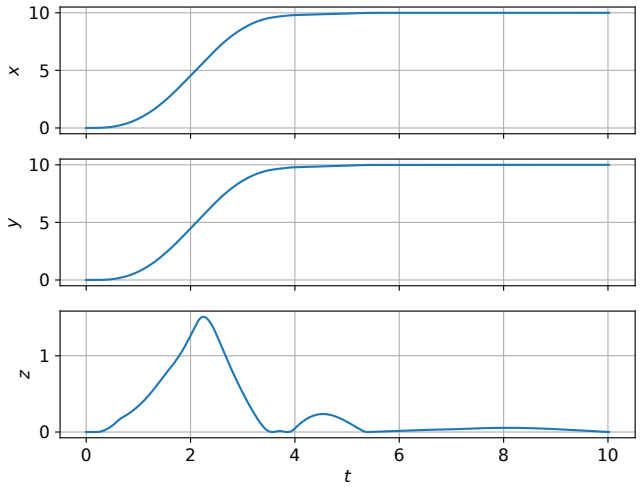

(a)

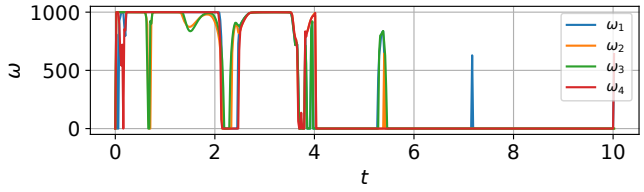

(b)

Fig. 1: Change of the position (a) and four motors angular velocity (b) of a UAV over the course of the trajectory, as it travels from $\boldsymbol{x}_0 = [0, 0, 0]^\top$ to $\boldsymbol{x}_f = [10, 10, 0]^\top$ as defined within Case 1. The UAV lands at its final destination at 4 s and remains there until t_f.

horizon. The resulting total energy consumption associated with the optimal trajectory is $E = 9.12$ kJ.

The solution took a total of 152.176 s to compute on a MacBook Pro (Apple M1, Cores: 8 (4 performance and 4 efficiency), Memory: 8 GB, 2020).

B. Case 2: Comparison To Literature

The proposed methodology is bench-marked against an example introduced in [2] which consists of a flight between $\boldsymbol{x}_0 = [0, 0, 0]^\top$ and $\boldsymbol{x}_f = [4, 5, 6]^\top$. The solution obtained in [2] is compared against the two formulations presented here:

1) The model, where dynamics of the z position is given by (6). This will be referred to as Air Energy Route Optimisation (AERO).
2) The model, where dynamics of the z position is given by (15). This will be referred to as Air Energy Route Optimisation with Landing Incentivisation (AERO-LI).

Here, the maximum number of iterations was set to 5,000. The results of this comparison are shown in Figure 2, 3 and 4.

Figure 2 compares three trajectories of the UAV in a 3D space, whilst Figure 3 gives the x, y and z components of the state over time. The trajectories given by the benchmark and AERO travel at a approximately constant cruise velocity

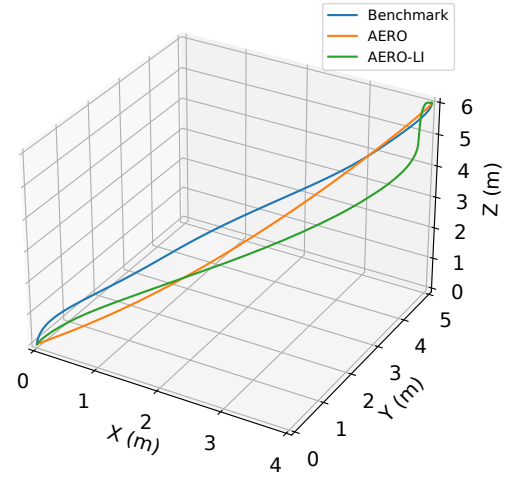

Fig. 2: The trajectories of three solutions: a benchmark solution in literature; the model presented in this paper but without landing incentives; and the model but with landing incentives, directly compared as they travel from $\boldsymbol{x}_0 = [0, 0, 0]^\top$ to $\boldsymbol{x}_f = [4, 5, 6]^\top$ as defined in Case 2.

with only minor changes in acceleration at the start and end of the journey. However, AERO-LI accelerates quickly at the start of the route and maintains a larger cruise velocity than in previous two solutions before beginning to decelerate near its destination. The arrival time for the benchmark and AERO is 20 s, whilst AERO-LI is able to reach its destination in a shorter time of approximately 4 s. The energy consumption for the three trajectories are 26.24 kJ for the benchmark, 26.35 kJ for AERO and 5.23 kJ for AERO-LI.

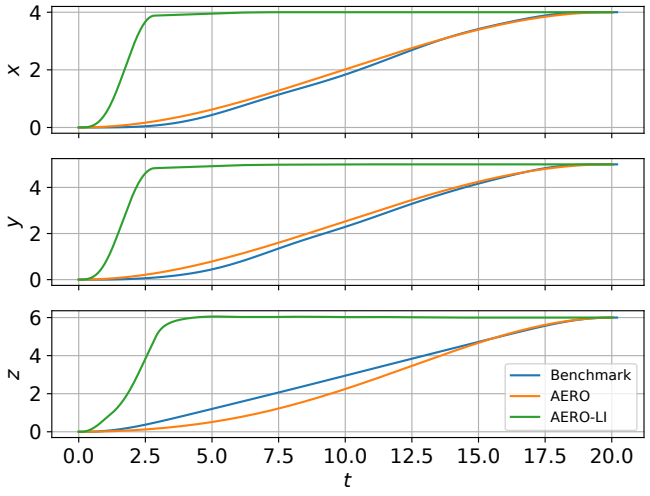

Fig. 3: The x, y and z spatial trajectories of all three models examined in Case 2 directly compared. The landing time of the third model can be seen at approximately 4 s, contrasted against the landing time of 20 s for the first and second models which don't include landing capabilities.

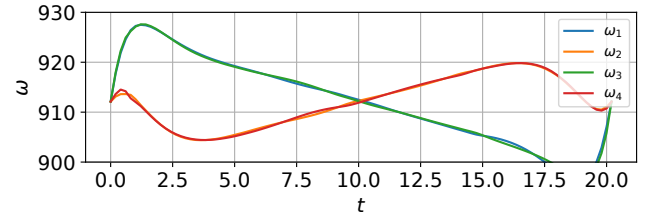

(a)

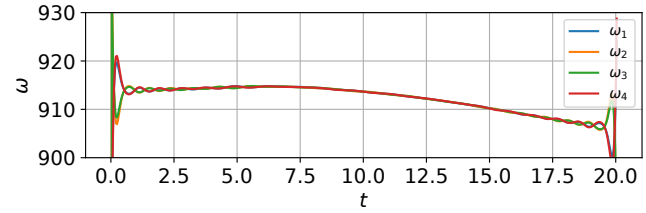

(b)

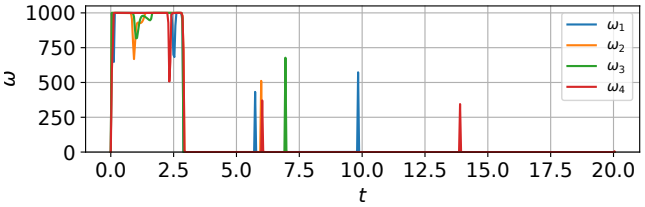

(c)

Fig. 4: Control input trajectories generated by (a) benchmark test presented in [2], (b) model presented in paper without landing capability and (c) model with landing capability for Case 2.

C. Case 3: NHS Logistics In The Solent Region Of The UK

Within the Solent region of the UK, the current BAU for the delivery of National Health Service (NHS) medical samples between surgeries and Southampton General Hospital (SGH) is the use of third party van-based couriers. Here, an example is presented which demonstrates the potential of incorporating UAVs into the logistics system. More precisely a route between the SGH and one of the surgeries, Hythe Hospital (HH), is analysed.

The start location is $\tilde{\boldsymbol{x}}_0 = [50.933°, -1.434°, 0]^\top$ and destination is $\tilde{\boldsymbol{x}}_f = [50.859°, -1.403°, 0]^\top$, where $\tilde{\boldsymbol{x}}$ is position vector given in [latitude, longitude, altitude] format, which is then converted to a UTM coordinate system [19] and then localised about the origin, so that $\boldsymbol{x}_0 = [0, 0, 0]^\top$ and $\boldsymbol{x}_f = [-2409.26, 8203.15, 0]^\top$. The maximum number of iterations was set to 10,000.

Figure 5 shows the top-down route generated by the model, for the trip between SGH and HH for both a UAV and a van. Figure 6 shows the time series of position and angular velocity of the motors of the UAV. It shows that the flight takes approximately 135 s, after which the UAV lands and uses the remaining allocated time to rotate itself to its final roll, pitch and yaw given by (21).

The total driven distance by a van is 16.4 km which was estimated using Google Maps to take approximately 27 min at an average speed of 36 km/h. The energy consumption

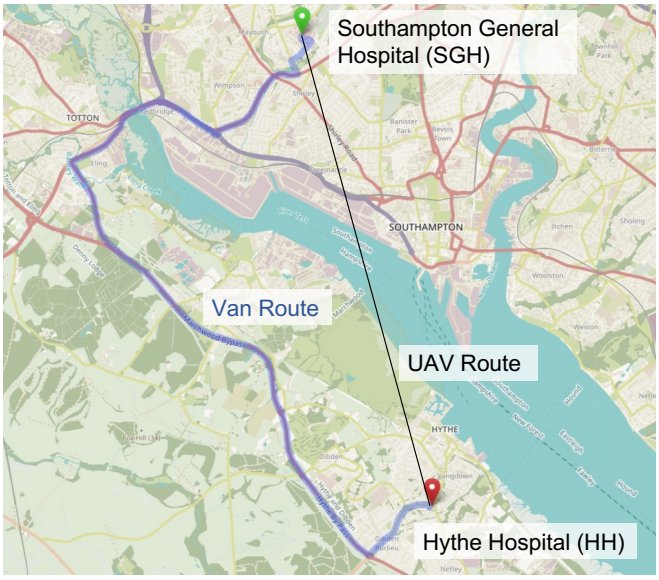

Fig. 5: Route taken by a UAV and a van in Case 3, travelling from SGH at $\tilde{\boldsymbol{x}}_0 = [50.933°, -1.434, °0]^\top$ to HH at $\tilde{\boldsymbol{x}}_f = [50.859°, -1.403°, 0]^\top$ [20].

for the van was calculated using the Comprehensive Modal Emission Model for a mass of 2,000 kg and assuming constant speed over trip duration. The energy consumption for the UAV flight was 179.60 kJ compared with the van route which results in 46.44 MJ. It should be noted that since van journey assumes constant speed, energy expenditure is underestimated. Nonetheless, even in this situation the potential energy and time savings from UAV utilisation can be demonstrated.

VI. DISCUSSION

Case 1 shows that the improved dynamical model has successfully incentivised the UAV to land at the final destination. This is a large improvement over previous methods as it allows the UAV to effectively minimise the energy usage by landing, instead of engaging in the redundant energy consuming maneuvers such as hover or prolonged level flight. Nonetheless, since the argument to the sigmoid function does not include rotational components, the UAV tends to slowly adjust its rotation once it reaches the destination. It is noted however, that the rotational adjustment is small in magnitude, with changes being no larger than $\pi/10$, and in practical applications a mechanism can be implemented to instantaneously achieve final orientation.

Figure 3 shows that in the Case 2 the optimisation model without the landing incentivisation closely resembles the benchmark trajectory despite a different algorithm used to obtain the solution, differences in the number of collocation nodes, the parameter ω_{max} and introduction of physical bounds on ϕ and θ to maintain values between $\pm\ \pi/10$

Also shown in Figure 3 is the improvement due to the landing incentive where the time taken to reach the destination is significantly smaller compared to the benchmark and the model without landing. This solution can be also

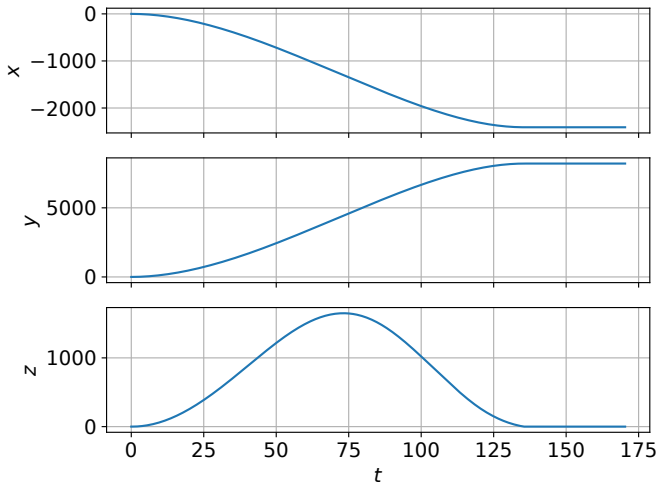

(a)

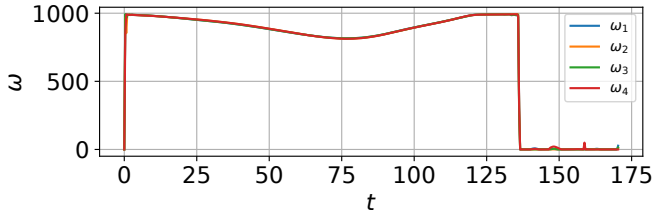

(b)

Fig. 6: Change of the position (a) and four motors angular velocity (b) of a UAV over the course of the trajectory, as it travels from $\boldsymbol{x}_0 = [0, 0, 0]^\top$ to $\boldsymbol{x}_f = [2409.26, 8203.15, 0]^\top$ as defined within Case 3. The UAV lands at its final destination at approximately 135 s and remains there until t_f.

considered to be more realistic based on the physical capabilities of the examined UAV. DJI Phantom 2 has an ascent speed of 6 m/s and a horizontal speed of 15 m/s [16]. For the trip which consists of the UAV ascending to a height of 6 m and moving horizontally by 6.4 m, a flight time of 4 s is closer to the time required to reach the destination if the DJI Phantom 2 was flying at its maximum speed. The improvement is further showed in Figure 4 where the area under the graph for $t > 7.5$ s is significantly smaller in Figure 4(c) than in Figure 4(a) and (b).

The application of the model to a real world in Case 3 shows an example where UAVs can be a viable replacement due to road network constraints imposed on land vehicles. Additionally the body of water that lies directly between SGH and HH further increases time and energy inefficiencies of the van route, whereas the UAV is able to fly directly between the two locations.

It is important to note, that payload considerations have not been taken into account when comparing UAVs to vans. UAVs have a very low payload capacity compared with a van therefore if multiple UAV trips are required to move samples from SGH to HH, the van quickly becomes more efficient. It must also be noted that further work is required to more realistically assess UAV viability in real-life applications. For example, a flight time of 135 s is only achievable as the body drag acting on the UAV is not included within the dynamics which allows it to reach high speeds. The top speed of the DJI Phantom 2 is 15 m\s [16]. Given the distance of the route is approximately 8.5 km, the journey should take approximately 9.5 minutes. Furthermore, wind over the Southampton Water could lead to conditions where this flight is far more energy intensive or even impossible. Similarly, the proposed solution does not take into account restrictions related to flying over certain higher risk areas and no fly zones, e.g., residential areas.

VII. CONCLUSIONS

This paper has introduced a landing capability and incentive which allows UAV minimum-energy route optimisation problems to obtain more optimal and realistic solutions, as they are no longer time dependant. This has been achieved by introducing a sigmoid function into the dynamics which reduces the effects of gravity to 0 at the final destination. This improvement has reduced travel time and energy consumption of a UAVs route by 80% when applied to a benchmark in literature. This has also allowed for longer distance route optimisation problems to be solved and so a comparison with other forms of transport can be produced.

A. Future Work

The omission of frontal drag acting on the body of the UAV and the effects of wind has lead to unrealistic results when routes are over larger distances, and this will be introduced to improve results. Furthermore, additional incentivisation will be implemented to ensure that the UAV can only land when its orientation matches its final roll, pitch and yaw. Similarly, dynamics of fixed-wing and hybrid UAVs will be modelled to enable the energy optimisation and assess potential capabilities of different UAV platforms within the logistics system. Lastly, the routes generated by the optimiser will be validated empirically to assess the accuracy of energy consumption and dynamical models.

B. Acknowledgment

Map data copyrighted OpenStreetMap contributors and available from https://www.openstreetmap.org.

REFERENCES

[1] T. Kirschstein, "Comparison of energy demands of drone-based and ground-based parcel delivery services," Transportation Research Part D: Transport and Environment, vol. 78:102209, 2020.

[2] F. Morbidi, R. Cano and D. Lara, "Minimum-energy path generation for a quadrotor UAV," 2016 IEEE International Conference on Robotics and Automation (ICRA), pp. 1492-1498, 2016.

[3] R. Alyassi, M. Khonji, S. C. K. Chau, K. Elbassioni, C. M. Tseng, and A. Karapetyan, "Autonomous recharging and flight mission planning for battery-operated autonomous drones," arXiv preprint arXiv:1703.10049, 2017.

[4] N. K. Ure, G. Chowdhary, T. Toksoz, J. P. How, M. A. Vavrina and J. Vian, "An automated battery management system to enable persistent missions with multiple aerial vehicles," IEEE/ASME Transactions on Mechatronics, vol 20(1): 275-286, 2015.

[5] S. Driessens and P. Pounds, "The Triangular Quadrotor: A More Efficient Quadrotor Configuration," IEEE Trans. Robot., vol 31(6): 1517– 1526, 2015.

[6] N. Kingry et al., "Design, Modeling and Control of a Solar-Powered Quadcopter," 2018 IEEE International Conference on Robotics and Automation (ICRA), pp. 1251-1258, 2018.
[7] J. Gong, T. -H. Chang, C. Shen and X. Chen, "Flight Time Minimization of UAV for Data Collection Over Wireless Sensor Networks," IEEE Journal on Selected Areas in Communications, vol. 36(9): 1942-1954, Sept. 2018.
[8] N. Kreciglowa, K. Karydis and V. Kumar, "Energy efficiency of trajectory generation methods for stop-and-go aerial robot navigation," 2017 International Conference on Unmanned Aircraft Systems (ICUAS), pp. 656-662, doi: 10.1109/ICUAS.2017.7991496, 2017.
[9] J. M. Moschetta, G. Hattenberger, and H. De Plinval, "Proceedings of the International Micro Air Vehicles Conference and Flight Competition 2017," IMAV, 2017.
[10] K. Dorling, J. Heinrichs, G. G. Messier and S. Magierowski, "Vehicle Routing Problems for Drone Delivery," IEEE Transactions on Systems, Man, and Cybernetics: Systems, vol. 47(1): 70-85, 2017.
[11] J. Zhang, J. F. Campbell, D. C. Sweeney II, and A. C. Hupman, "Energy consumption models for delivery drones: A comparison and assessment," Transportation Research Part D: Transport and Environment, vol. 90:102668, 2021.
[12] R. D'Andrea, "Guest Editorial Can Drones Deliver?," IEEE Transactions on Automation Science and Engineering, vol. 11(3): 647-648, 2014.
[13] Z. Liu, R. Sengupta and A. Kurzhanskiy, "A power consumption model for multi-rotor small unmanned aircraft systems," 2017 International Conference on Unmanned Aircraft Systems (ICUAS), pp. 310-315, 2017.
[14] S. Bouabdallah, P. Murrieri, and R. Siegwart, "Towards autonomous indoor micro VTOL. Autonomous robots," vol. 18(2):171-183, 2005.
[15] F. Ahmad, P. Kumar, A. Bhandari, and P. P. Patil, "Simulation of the quadcopter dynamics with LQR based control," Materials Today: Proceedings, vol. 24: 326-332, 2020.
[16] DJI Phantom 2 specifications webpage. https://www.dji.com/uk/phantom-2/info.
[17] M. Kelly, "An introduction to trajectory optimization: How to do your own direct collocation," SIAM Review, vol. 59(4):849-904, 2017.
[18] A. Wächter, L. T. Biegler, "On the implementation of an interior-point filter line-search algorithm for large-scale nonlinear programming," Mathematical Programming, vol. 106: 25–57, 2006.
[19] R. Welch, A. Homsey, "Datum shifts for UTM coordinates," Photogrammetric engineering and remote sensing, vol. 63(4): 371-375, 1997.
[20] OpenStreetMap contributors. (2015) Planet dump retrieved from https://planet.openstreetmap.org.